Science of Sintering, **54** (2022) 211-221

https://doi.org/10.2298/SOS2202211V

UDK: 546.284; 692.533.1; 539.53

Mechanical Properties of Biomass-derived Silica Nanoparticles Reinforced PMMA Composite Material

Marija M. Vuksanović[1*)], Ivana O. Mladenović[2], Nataša Z. Tomić[3], Miloš Petrović[4], Vesna J. Radojević[4], Aleksandar D. Marinković[4], Radmila M. Jančić Heinemann[4]

[1]University of Belgrade, Department of Chemical Dynamics and Permanent Education, „VINČA" Institute of Nuclear Sciences - National Institute of the Republic of Serbia, Mike Petrovića Alasa 12-14, 11351 Belgrade, Serbia

[2]University of Belgrade, Institute of Chemistry, Technology and Metallurgy, National Institute of the Republic of Serbia, Njegoševa 12, 11000 Belgrade, Serbia

[3]Innovation Centre of Faculty of Technology and Metallurgy in Belgrade, Karnegijeva 4, 11000 Belgrade, Serbia

[4]University of Belgrade, Faculty of Technology and Metallurgy, Karnegijeva 4, 11120 Belgrade, Serbia

Abstract:

Rice husk was used to produce silica particles, which were then used to reinforce the polymer matrix. The synthesized SiO_2 particles were characterized using X-ray diffraction, Fourier transforms infrared spectroscopy (FTIR) and scanning electron microscopy with EDS. In a PMMA matrix, prepared SiO_2 particles in amounts of 1, 3, and 5 wt.% were used as reinforcing agents. The goal of this research was to see if SiO_2 particles had any effect on the mechanical properties of polymer composite materials. The morphology of the composites was examined using a field emission scanning electron microscope (FE-SEM). Vickers microindentation hardness and impact testing were used to determine the mechanical properties of the obtained composites. The indentation creep's behavior of a polymethylmetacrylate (PMMA) composite material with varying amounts of nanoparticles (SiO_2) was investigated and analyzed.

Keywords*: Silica; Composites; Vickers hardness; Creep behavior.*

1. Introduction

Poly-methylmethacrylate (PMMA) has a semi-crystalline structure and is an amorphous polymer [1], it is a widely used artificial polymer that has garnered considerable attention due to its physical, optical, electrical, thermal, and mechanical properties [2]. PMMA is a clear, colorless, amorphous, transparent thermoplastic with bulky side groups that softens when heated. PMMA has excellent thermal stability, high tensile strength [3,4] and excellent optical clarity, making it particularly useful in applications where light transmission is critical. When the properties of polymers are insufficient to meet the needs, fillers and reinforcements are added creating polymer composites [5]. This is accomplished by preparing and synthesizing composite materials with properties that are completely or partially different

*) **Corresponding author:** marija.vuksanovic@vin.bg.ac.rs

from all of their constituent materials. As a result, composite materials have various, improved, and enhanced physical and chemical properties. For example, if one material is sufficiently strong and another is highly flexible, combining them creates a new type of material (called a composite material) with greater strength and flexibility [6]. Because of its wide range of applicability, silica has been cited in the literature as filler in polymers. Silica is one of the most abundant materials on the planet, found in sand and quartz, and it can be synthesized through chemical reactions. One source of silica is rice husk because the rice plant requires more chemical elements during its growth, including silicon, which plays important role in rice plant growth, such as developing resistance to specific stresses and diseases [7]. The plant synthesized silica has very fine structure and does not demand the use of polluting aggressive chemicals for production being the green source for this important product. The majority of rice husks are burned or discarded into the environment, the value of this agricultural by-product rises with the use of rice husks as a source of silica.

Polymer-silica nanocomposites with enhanced physical and mechanical properties have a wide range of applications, including coatings [8,9], flame retardant materials [10], optical devices [11], packaging materials [12], photoresist materials [13], photoluminescent conducting film [14], pervaporation membranes [15], proton exchange membrane [16], grouting materials [17], sensors [18], and others.

The creep is one of important features of polymeric composites, such as PMMA with SiO_2 particles because it occurs at ambient conditions. Investigations and analysis of this specific mechanical behavior provide information related to the time-dependent flow of materials, i.e., determination of the creep resistance of polymeric composite material [19–21]. The creep response of PMMA composites containing micro and nanosized carbon filaments was investigated with variation time and temperature range in the literature [19]. With the addition of the fillers, the creep strain decreases, which means that the composite material with filaments as reinforcement presents a lower creep strain than the clean PMMA [22]. Particles small size and good dispersion in the PMMA matrix affect the strengthening of the composite, which result in greater hardness and creep resistance, which will be shown in the paper [23,24]. The effect of nanoparticles on reinforcing the PMMA matrix is to inhibit crack initiation, and this was also observed during the micro indentation test. In this sense, the creep behavior is of relevance because it predicts the occurrence of cracking of thermoplastic polymer [25]. The incorporation of nanoparticles in the polymer matrix has restricted the mobility of the polymer chain and with the incorporation of smaller nanoparticles, the creep resistance was greater [25].

There is a number of studies combining nanoindentation creep measurements with viscoelastic theoretical models for polymers [26,27]. Creep behavior of PMMA was investigated using nanoindenter [28], AFM-indent technique and compression test to study creep and compare different measurement methods, with the suggestion that the methods can be applied to determine changes in creep behavior due to material degradation. The indentation creep method represents a simple, quick, and non-destructive method for an investigation of the mechanical behavior of different composite systems. The effects of hydrothermal aging on indentation creep measurements of PMMA was studied and found that creep displacement increase with aging time [28].

Indentation creep behavior of composite material consisting of polymethylmetacrylate (PMMA) with different amounts of plant produced nanoparticles (SiO_2) was studied and analyzed. The objective was to determine the role of the addition of SiO_2 nanoparticles in the thermoplastic polymer (PMMA).

2. Materials and Experimental Procedures

2.1 Materials and methods

The auto polymerizing set for denture base Akrilat – R serves as the source of the PMMA matrix (Laser Dental Products). Rice husks were obtained from the Levidiagro rice producer in Kocani, North Macedonia. Sulfuric acid, obtained from Zorka Sabac, was used as a chemical.

2.2 Preparation of Silica particles from rice husk

The rice husk was first washed with water and dried to remove pollution. The obtained husk (100 g) was treated with 10 % sulfuric acid and heated at 80^{o}C for 3 h. The husk was then washed with distilled water until the pH reached 7. After the acid was removed, the husks were dried at 50^{o}C. The obtained product was black and contained the remains of the organic products after being treated with the Bunsen flame. The final step was a 4-hour heat treatment in an oxidative atmosphere at 800^{o}C. This was the final step, and the resulting product was used in further experiments.

2.3 Preparation of PMMA composites reinforced with silica particles

The auto polymerizing set for denture base preparation was used as the source of the PMMA matrix. The prepolymerized powder and monomer liquid were included in the set. The producer stipulated that the powder-to-liquid volume ratio be 2.5:1. The polymerization process was carried out at room temperature. The PMMA matrix was used to prepare composites with additions of 1, 3, and 5 wt.% of reinforcement. An ultrasonic bath was used to disperse the obtained silica particles in a monomer (liquid) component. The ultrasonication lasted 30 min to avoid agglomeration and achieve good dispersion. The powder component (PMMA) was added to the liquid, resulting in a paste that was then placed in an aluminum alloy mold. For comparison, a pure polymer PMMA sample was also prepared.

2.4 Material characterization

The particles' morphology and shape were examined using a Mira3 Tescan field emission scanning electron microscope (FE-SEM) set to 20 kV. A thin gold film had previously been deposited on the samples surface. The morphology of the composite materials was examined using an (FE-SEM) at 3 kV.

An Ital Structure APD2000 X-ray diffractometer was used to identify crystal phases of silica in a Bragg–Brentano geometry using CuK radiation (λ = 1.5418) and step-scan mode (range: 10-90° 2, step-time: 0.50 s, step-width: 0.02°). FTIR spectra of SiO_2 fillers and composite materials were collected using a Nicolet 6700 spectrometer (Thermo Scientific) in the attenuated total reflectance (ATR) mode with a single bounce 45 °F Golden Gate ATR accessory with a diamond crystal and an electronically cooled DTGS detector. The spectra were ATR corrected co-additions of 64 scans at 4 cm^{-1} spectral resolution. The OMNIC software was used on the Nicolet 6700 FTIR spectrometer, which recorded spectra in the wavelength range of 2.5 to 20 μm (i.e., 4000 cm^{-1} to 400 cm^{-1}). The dwell time was 25 seconds, and the applied load was 4.9 N, for determining the composite hardness of the material. The indentation was created using a Vickers tester, model “Leitz Kleinert Prufer DURIMET I.” (Leitz, Oberkochen, Germany). An optical microscope (Olympus CX41) connected to a computer with image software was used to measure the diagonal size of the indents. The number of indents was three, and the hardness was calculated using the

arithmetic mean of the diagonal. The composite hardness values were computed using Eq. 1 [29]:

$$H_c A = \frac{1.8544 \cdot P}{d^2} \qquad (1)$$

where P is the applied load (in N), the constant 1.8544 is a geometrical factor for the Vickers pyramid, d is the average diagonal length of the indent (in m).

Creeping indentation of the PMMA/SiO_2 composites' properties were investigated by measuring the composite hardness with a variation of dwell time (5-30 s), with step 5 s, at fixed applied loads, P of 0.49 and 4.9 N at room temperature. When a higher indentation load was applied, a large plastic deformation zone around the indents as well as cracking of the material near the impression was observed. Furthermore, because the ISE (Indentation Size Effect) effect is more dominant than the creep mechanism, these measurements were not considered. Constant applied indentation load (0.49N) and a variable dwell time during the indentation process for the creep analysis were used; Indentation testing of PMMA/SiO_2 composite samples was carried out at room temperature.

The results of hardness measurements were used for the creep mechanism specification through calculation of the creep parameter, named- stress exponent μ of the samples of PMMA with different content of nano-silica particles, according to the model of Sargent-Ashby (S-A) [30]. Eq. (2) gives the relation between the time-dependent composite hardness H_c and stress exponent μ as:

$$H_c = \frac{\sigma_0}{c \cdot \mu \cdot t} \qquad (2)$$

where ε_0 is the strain rate at reference stress σ_0, c is constant, t is dwell time and μ is the stress exponent [30,31].

The plots of lnH_c against ln$t$ give straight lines whose slopes are equivalent to the negative inverse stress exponent (-1/μ). Based on the value of the exponent, μ, it is possible to estimate the material creep mechanism based on the theoretical model S-A and Eq. (2).
The composites' impact energy tests were carried out on the Shimadzu, High-Speed Puncture Impact testing machine HYDROSHOT HITS-P10. Total absorbed energy was calculated following the load-time diagram, providing energy values for the maximum load and puncture point. The puncture point was defined as the point at which the force becomes zero. According to previous experience [7], the striker with a hemispherical head (diameter 12.7 mm) was loaded with the programmable impact velocity set at 1 m/s. The sampling time was 10 μs and 12000 points were collected, some before and most during and after the impact. The striker was programmed to puncture all of the samples under consideration. The measurement was performed on three specimens from each group, and the results were presented as the mean values of the three tests.

3. Results and Discussion

Fig. 1a depicts the XRD diffractogram of silica particles synthesized from rice husk. Fig. 1b shows FESEM microphotographs used to examine the morphology of the obtained particles. The diffractogram depicts the spectrum of a non-crystalline solid material with no crystalline structure, implying that the material obtained is a non-crystalline powder. The diameters of the obtained silica particles from rice husk were previously published [32] in the range of 10-233 nm, indicating that the majority of the silica particles are nanoparticles.

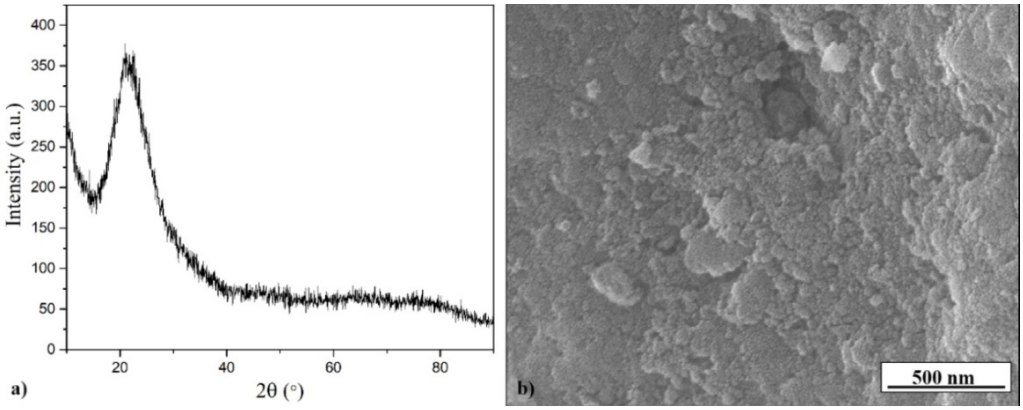

Fig. 1. a) XRD pattern and b) SEM micrograph of silica particles from rice husk.

Fig. 2. shows the FTIR spectrum of SiO_2 particles, pure matrix, and composite material.

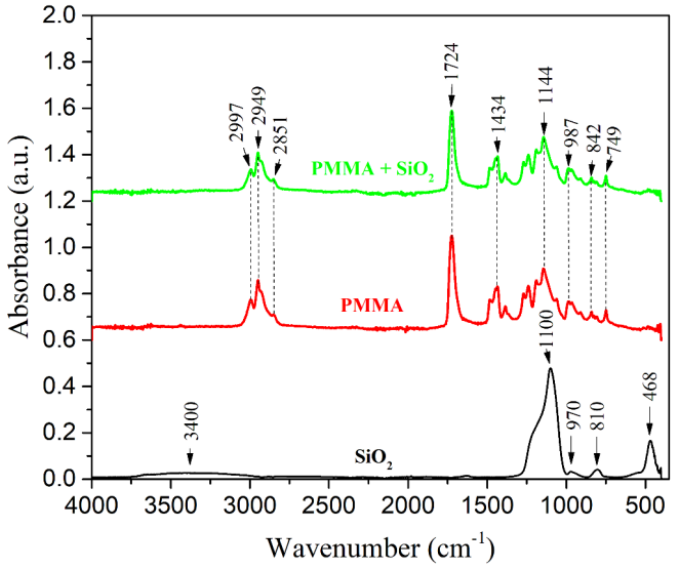

Fig. 2. FTIR of SiO_2, pure matrix and composite material.

At around 3384 cm^{-1}, the FTIR spectra show absorption bands caused by stretching and in-plane bending vibrations of the OH group of molecular H_2O [33]. The silica particle characteristic peaks at 970, 810 and 468 cm^{-1} are well visible in the spectrum. Absorption peaks 1100 cm^{-1} and 810 cm^{-1} have been assigned to the antisymmetric and symmetric vibrations of the Si–O–Si elongation, respectively. The vibration bending of the Si–O–Si bond was linked to the absorption peak at 468 cm^{-1} [34]. PMMA has characteristic peaks at 1724 cm^{-1} ν (C = O) and 1434 cm^{-1} ν (C - O). The bands at 2997, 2949, and 2851 cm^{-1} correspond to the methyl group's C-H elongation (CH_3). The vibrations of the ester group C - O correspond to the peak at 1144 cm^{-1} while the elongation ranges C - C are at 987 and 749 cm^{-1} [35].

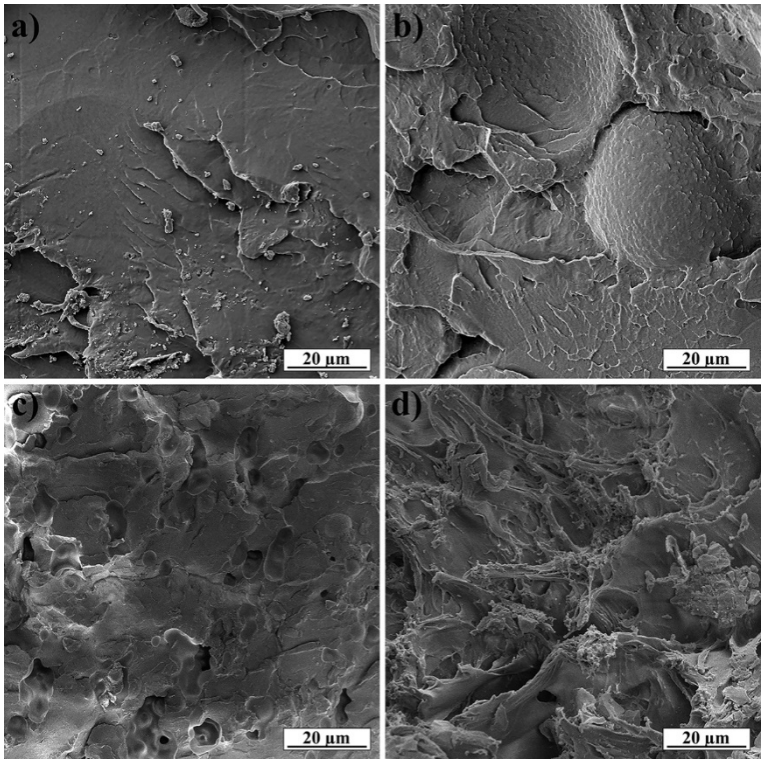

Fig. 3. SEM micrographs of a cross-section of the a) pure matrix and composite after fracturing with b) 1 wt.%, c) 3 wt.% and d) 5 wt.% of SiO_2 fillers.

SEM micrographs were obtained from the cross-section of the specimen obtained after mechanical testing, Fig. 3.

The microhardness testing of pure PMMA and composite material was done on a Vickers device with (4.9 N) and a dwell time of 25 s. The results are shown in Fig. 4. Those measurements prove that the hardness is increasing with the addition of the reinforcement from 142 MPa, which was the value for the pure matrix to the value of 156 MPa that was achieved with the addition of 5 wt.% of the reinforcements. The overall increase of the hardness was about 10% for the addition of 5 wt.% of the reinforcement.

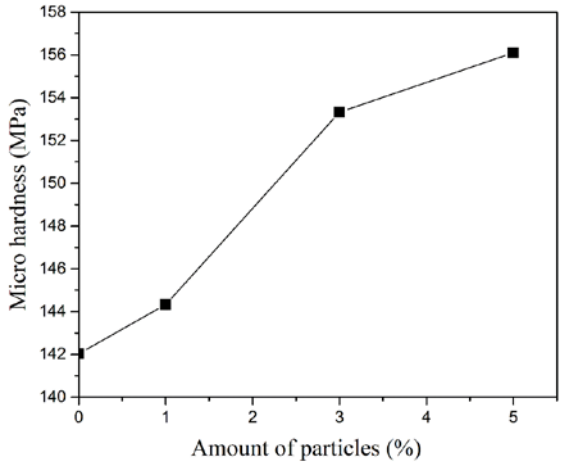

Fig. 4. Vickers hardness of composite materials with SiO_2 particles.

Indentation results are expressed as a variation of the composite hardness values, H_c, with a dwell time (t) at the applied load of 0.49 N for PMMA samples obtained with mixing different weight % of silica particles. Figure 5a shows the experimental data of composite hardness changing with dwell time variation, fitted according to the Sargent-Ashby model to determine the creep parameter. Stress exponent values are expected to indicate the dependence of the creep behavior on the amount of silica particles in the PMMA matrix, because of a change in the structure of the composite. The factor describing the creep behavior changes with addition of silica reinforcement as it is shown in Fig. 5b.

Indentation experiments have shown that a further increase in the indentation depth (increase the diagonal size of indent) occurs overtime at the same maintained load, which means that the composite hardness decreases with the increase of the dwell time. Microhardness of PMMA without silica particles in the matrix is lower than PMMA/SiO_2 composite, because that the particles included in the polymer matrix of PMMA provide resistance to penetration of indenter materials. The behavior of the composite hardness of the PMMA/SiO_2 composite with the change of the indentation time (dwell time) can be described by the power function. The highest creep resistance is shown by the sample with 5 wt.% of silica particles, and the lowest by the PMMA sample without reinforcement. This behavior of composite can be explained through the sliding mechanism, each particle boundary of silica particles acts as a mini barrier during polymer creep of PMMA matrix during indentation.

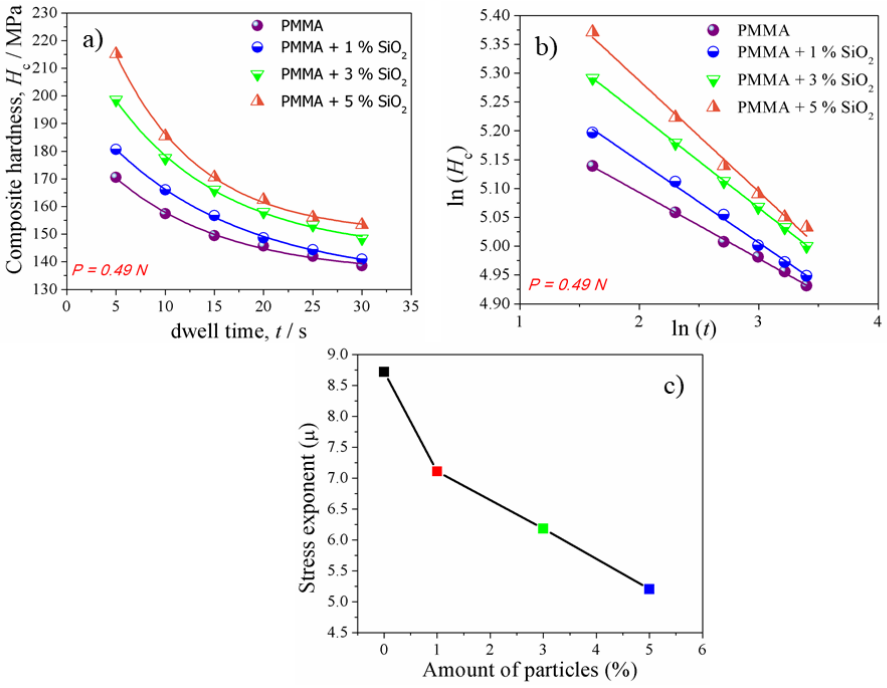

Fig. 5. Variation of the composite hardness of the PMMA/SiO_2 composite as a function of dwell time during micro indentation a) Vickers testing at constant load 0.49 N, b) fitting experimental data of indentation according to Sargent-Ashby model, and c) dependence stress exponent vs. amount of SiO_2 particles in PMMA.

A plot of ln (Hc) against ln (t) gives a linear plot (Fig. 5b) and by applying linear regression to the data set, at the value of the creep exponent, μ is calculated. The values of the calculated stress exponent μ for all composite samples are given in Table I. The dependence of the stress exponent on the content of silica particles in the composite is given in Fig. 5c.

Tab. I Fitting results obtained according to data in Fig. 5b. The values of stress exponents for the PMMA/SiO_2 composite obtained with various amounts of silica particles in PMMA matric, at a constant indentation load 0.49 N, are given.

Wt.% of SiO_2 in PMMA matrix	Slope (k)	Intercept (n)	Stress exponent (μ)
0	-0.1147	5.3225	8.7184
1	-0.1407	5.4291	7.1073
3	-0.1618	5.5517	6.1805
5	-0.1923	5.6716	5.2002

The optical microscopy image showing Vickers hardness indentation in the PMMA polymer matrix with 1 wt.% of SiO_2 particles, an applied load of 0.49 N and a dwell time of 25 s is given in Fig. 6a. Fig. 6b is a view of a Vickers imprint on the top surface of a mechanically prepared pure PMMA sample without silica particles at a dwell time of 30 s and 0.49 N applied load. Based on Figs 6a and 6b the volumes of the deformation zone around the indents are quite different. The deformation zone of a particle-reinforced PMMA sample is smaller than the deformation zone for a pure PMMA sample. This behavior is expected because each nanoparticle of SiO_2 incorporated into the polymer matrix provides additional resistance when the diamond indenter penetrates in the volume of the composite material. In addition, the dwell time of the indenter is shorter for composite material. The elastic recovery of pure PMMA decreases with increasing indentation duration at 30 s. Due to the possible discontinuous distribution of silica nanoparticles in the polymer matrix, a slight asymmetry in the diagonal size is observed (Fig. 6a).

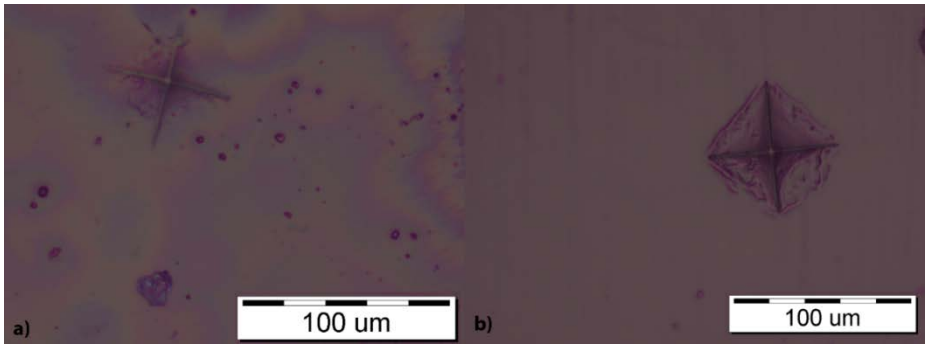

Fig. 6. Vickers hardness indentation made by microhardness tester in the PMMA polymer matrix at applied indentation load of 0.49 N: a) PMMA with 1 wt.% of SiO_2 and dwell time at 25 s and b) without SiO_2 and dwell time at 30 s.

In this investigation, the values of the stress exponent, μ obtained at the load 0.49 N, ranging from 5.20 to 8.72. The value of this exponent increases with decreasing wt.% of SiO_2 particles. The lowest creep resistance is observed in the PMMA sample without reinforcement. This was followed by a sample with a minimal amount of silica particles. The most resistant to creep is the sample with the maximum content of silica particles that were in this case 5 wt.%. The exponent in metallic materials signifies the creep mechanism. The value of exponent around 1 means that diffusion creep was the dominant creep mechanism, if the value of $\mu \approx 2$ the creep mechanism is a grain boundary sliding, and if the value of μ is in the range between 3-10, mechanism of indentation deformation will be dislocation climbs and dislocation creep [36,37]. In composite materials, the mechanism of viscoelastic behavior can be explained differently. The presence of small particles, such as silica, used in observed specimens acts on the ability of the polymer chains to move. Silica particles are known to have some active sites on their surface enabling the bonding to the polymer matrix and

therefore they act as bridges that inhibit the movement of the matrix material and make the viscoelastic deformation slower. This behavior is mostly due to the presence of OH groups on the surface of the silica particles observed on the FTIR analysis. It was previously shown that the form of alumina particles influences the behavior of the composite and that there was some interaction of those particles with the matrix. In the case of alumina particles the presence of OH bonds is less present and less relevant but it enables the interaction with the matrix [38,39]. However, the presence of the OH groups on the surface of silica particles is much more present as proven in the FTIR spectrum so they exhibit the good ability to create bonds with the matrix and to influence the deformation of the composite behavior.

Fig. 7. shows the results of the impact testing of prepared composite materials. In impact testing, the energy is transferred to the specimen in an extremely short time and the material absorbs this energy before fracture. The composites having more reinforcements are exhibiting more resistance to the impact testing and absorb more energy during this testing. This can be contributed to the presence of silica particles in the structure and their ability to build bonds with the matrix and to make the material destruction more difficult. The performance of the material is getting better with the addition of the silica to the composite in terms of material stiffness. The content of reinforcement is limited as the higher amounts of reinforcement are responsible for the agglomeration of particles. The addition of larger amount of particles makes the product that is very difficult to process, and the agglomeration ruins the good composite properties.

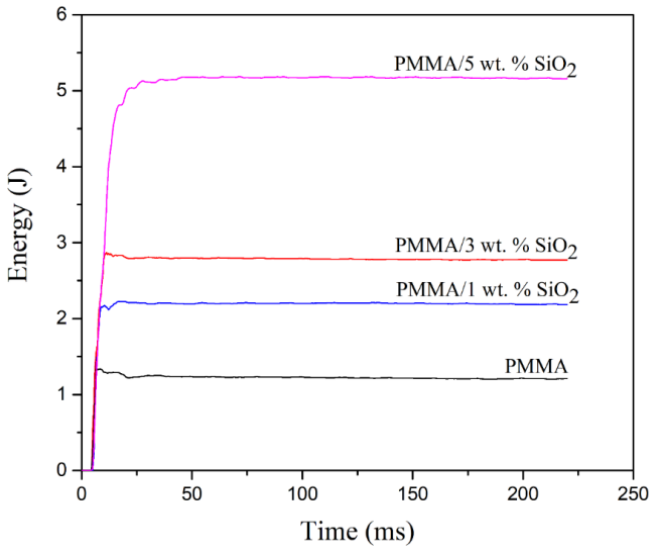

Fig. 7. Energy absorption of composites reinforced with SiO_2 particles during impact testing as a function of time and reinforcement content.

4. Conclusion

Plant derived silica particles were noncrystalline and exhibited the presence of OH groups on the surface as proved by XRD and FTIR analysis. Those particles were used as reinforcements in the composite materials in 1 wt.%, 3 wt.% and 5 wt.% to reinforce the PMMA matrix. Vickers micro-hardness test proved that the addition of reinforcement increases the composite's hardness. The viscoelastic behavior was modified with the presence of the reinforcement in the material and the addition of silica particles improves the creep resistance as measured in the time-dependent indentation experiments. Toughness was measured using a high-speed impact tester, and the results show that adding reinforcement to

the material results in a significant improvement. The toughness of the sample containing 5 wt.% SiO_2 particles have the highest absorbed energy when compared to the matrix.

Acknowledgments

The Ministry of Education, Science and Technological Development of the Republic of Serbia funded the research. (Contracts No.451-03-68/2021-14/200135, 451-03-68/2021-14/ 200287, and 451-03-9/2021-14/200026).

5. References

1. S. Choudhary, R. J. Sengwa, J. Appl. Polym. Sci. 132(3) (2015) 41311.
2. S. Rattan, P. Singhal, A. L. Verma, Polym. Eng. Sci. 53(10) (2013) 2045-2052.
3. George Odian, Principles of Polymerization, John Wiley & Sons, Inc., Hoboken, NJ, USA, n.d., pp. 619-728.
4. V. Malisic, N. Tomic, M. Vuksanovic, B. Balanc, Z. Stevic, A. Marinkovic, R. Jancic-Heinemann, S. Putic, Sci. Sinter. 52(4) (2020) 457-467.
5. S. Perisic, M. Vuksanovic, M. Petrovic, A. Radisavljevic, A. Grujic, R. Jancic-Heinemann, V. Radojevic, Sci. Sinter. 51(1) (2019) 115-124.
6. P. Meneghetti, S. Qutubuddin, A. Webber, Electrochim. Acta 49(27) (2004) 4923-4931.
7. M. Sahebi, M. M. Hanafi, A. Siti Nor Akmar, M. Y. Rafii, P. Azizi, F. F. Tengoua, J. Nurul Mayzaitul Azwa, M. Shabanimofrad, Biomed Res. Int. 2015 (2015) 1-16.
8. P. Hammer, F. C. dos Santos, B. M. Cerrutti, S. H. Pulcinelli, C. V. Santilli, Prog. Org. Coatings 76(4) (2013) 601-608.
9. V. A. Soloukhin, W. Posthumus, J. C. Brokken-Zijp, J. Loos, G. de With, Polymer (Guildf). 43(23) (2002) 6169-6181.
10. S. Kim, C. A. Wilkie, Polym. Adv. Technol. 19(6) (2008) 496-506.
11. C.-C. Chang, W.-C. Chen, Chem. Mater. 14(10) (2002) 4242-428.
12. Y. Sun, Z. Zhang, K.-S. Moon, C. P. Wong, J. Polym. Sci. Part B Polym. Phys. 42(21) (2004) 3849-3858.
13. J.-D. Cho, H.-T. Ju, Y.-S. Park, J.-W. Hong, Macromol. Mater. Eng. 291(9) (2006) 1155-1163.
14. X. Li, X. Li, G. Wang, Mater. Lett. 60(28) (2006) 3342-3345.
15. S. Das, A. K. Banthia, B. Adhikari, Desalination 197(1–3) (2006) 106-116.
16. Y.-S. Ye, J. Rick, B.-J. Hwang, Polymers (Basel). 4(2) (2012) 913-963.
17. X. J. Xiang, J. W. Qian, W. Y. Yang, M. H. Fang, X. Q. Qian, J. Appl. Polym. Sci. 100(6) (2006) 4333-4337.
18. Y. Su, React. Funct. Polym. 66(9) (2006) 967-973.
19. H. Varela-Rizo, M. Weisenberger, D. R. Bortz, I. Martin-Gullon, Compos. Sci. Technol. 70(7) (2010) 1189-1195.
20. H.G.M. Doan, P. Mertiny, Materials (Basel). 13(20) (2020) 4637.
21. X. Hao, H. Zhou, Y. Xie, Z. Xiao, H. Wang, Q. Wang, Polym. Compos. 40(4) (2019) 1576-1584.
22. H. Varela-Rizo, M. Weisenberger, D. R. Bortz, I. Martin-Gullon, Compos. Sci. Technol. 70(7) (2010) 1189-1195.
23. G. A. Lazouzi, M. M. Vuksanović, N. Tomić, M. Petrović, P. Spasojević, V. Radojević, R. Jančić Heinemann, Polym. Compos. 40(5) (2019) 1691-701.
24. G. Lazouzi, M. M. Vuksanović, N. Z. Tomić, M. Mitrić, M. Petrović, V. Radojević, R. J. Heinemann, Ceram. Int. 44(7) (2018) 7442-7449.

25. O. Starkova, J. Yang, Z. Zhang, Compos. Sci. Technol. 67(13) (2007) 2691-2698.
26. M. L. Oyen, Acta Mater. 55(11) (2007) 3633-3639.
27. P. Christöfl, C. Czibula, M. Berer, G. Oreski, C. Teichert, G. Pinter, Polym. Test. 93 (2021) 106978.
28. L. Lv, H. Lin, T. Jin, Polym. Test. 93 (2021) 106991.
29. ASTM International, West Conshohocken, PA (2016). 10.1520/E0384-16.
30. S. P. M., M.F. Ashby, Mater. Sci. Technol. 8(7) (1992) 594-601.
31. I. O. Mladenović, N. D. Nikolić, J. S. Lamovec, D. Vasiljević-Radović, V. Radojević, Metals (Basel). 11(1) (2021) 111.
32. N. Z. Tomić, A. D. Marinković, B. Balanč, V. Obradović, V. Pavlović, V. Manojlović, M. M. Vuksanović, Iran. Polym. J. 30 (2021) 319-330.
33. N. Yan, F. Wang, H. Zhong, Y. Li, Y. Wang, L. Hu, Q. Chen, Sci. Rep. 3(1) (2013) 1568.
34. S. H. Kwon, I. H. Park, C. M. Vu, H. J. Choi, J. Taiwan Inst. Chem. Eng. 95 (2019) 432-437.
35. S. Ahmad, S. Ahmad, S.A. Agnihotry, Bull. Mater. Sci. 30(1) (2007) 31-35.
36. B. Walser, O. D. Sherby, Scr. Metall. 16(2) (1982) 213-219.
37. S. Farhat, M. Rekaby, R. Awad, SN Appl. Sci. 1(6) (2019) 546.
38. S. A. Ben Hasan, M. M. Dimitrijević, A. Kojović, D. B. Stojanović, K. Obradović-DethURIČIĆ, R. M. Jančić Heinemann, R. Aleksić, J. Serbian Chem. Soc. 79(10) (2014) 1295-1307.
39. F. A. Alzarrug, M. M. Dimitrijević, R. M. Jančić Heinemann, V. Radojević, D. B. Stojanović, P. S. Uskoković, R. Aleksić, Mater. Des. 86 (2015) 575-581.

Сажетак: *Љуска пиринча је коришћена за производњу честица силицијум диоксида, које су коришћене за ојачавање полимерне матрице. Синтетизоване честице силицијум диоксида карактерисане су дифракцијом рендгенских зрака, инфрацрвеном спектроскопијом Фуријеове трансформације (ФТИР) и скенирајућом лектронском микроскопом са ЕДС. У матрици полиметил метакриилата, припремљене честицее силицијум диоксида у количинама од 1, 3 и 5 мас. %, коришћене су као ојачање. Циљ овог истраживања био је да се утврди да ли честице силицијум диоксида утичу на механичка својства полимерних композитних материјала. Морфологија композита је испитивана коришћењем поља емисионог скенирајућег електронског микроскопа (ФЕ-СЕМ). За одређивање механичких својстава добијених композита коришћени су Вицкерс микроиндентациони тестови и испитивање на удар. Понашање пузања композитног материјала полиметилметакрилата (ПММА) са различитим количинама наночестица силицијум диоксида је испитано и анализирано.*

Кључне речи*: Силицијум диоксид, композити, тврдоћа по Викерсу, creep behavior, понашање пузања.*